

## Mixed Convection Boundary Layer Flow over a Solid Sphere in $Al_2O_3-Ag$ /Water Hybrid Nanofluid with Viscous Dissipation Effects

Eddy Elfiano<sup>1,2</sup>, Nik Mohd Izual Nik Ibrahim<sup>2,\*</sup>, Muhammad Khairul Anuar Mohamed<sup>3</sup>

<sup>1</sup> Department of Mechanical Engineering, Faculty of Engineering Universitas Islam Riau, 28284 Pekanbaru, Provinsi Riau, Indonesia

<sup>2</sup> Faculty of Engineering and Technology DRB-HICOM University of Automotive Malaysia, Peramu Jaya Industrial Area, 26070 Pekan, Pahang, Malaysia

<sup>3</sup> Centre for Mathematical Sciences Universiti Malaysia Pahang, Lebuhraya Persiaran Tun Khalil Yaakob, 26300 Kuantan, Pahang, Malaysia

### ARTICLE INFO

#### Article history:

Received 17 March 2024

Received in revised form 16 April 2024

Accepted 18 May 2024

Available online 30 June 2024

#### Keywords:

Mixed convection; Hybrid nanofluid;  
Sphere; Viscous dissipation

### ABSTRACT

The current study aims to investigate how heat transfer and skin friction develop by modifications in the fundamental advantages of fluids in the presence of mixed convection boundary layer flow over on a sphere in hybrid nanofluids. Hybrid nanofluids have superior thermophysical characteristics compared to conventional heat transfer fluids such as oil, water, and ethylene glycol, as well as mono nanofluids, in thermal processes. The numerical solutions for the reduced Nusselt number, local skin friction coefficient temperature profile, and velocity profiles are discovered and clearly presented. The Eckert number, the mixed convection parameter  $\lambda$ , and the nanoparticle volume fraction are all investigated and described. It is found that increasing the volume percentage of nanomaterial in nanofluid enhanced the value of the skin friction coefficient. The low density of nano oxides in hybrid nanofluids, such as alumina, also contributes to reduced friction between fluid and body surface. The findings of a computational investigation demonstrate that the use of a hybrid nanofluid, composed of nanometal and nano-oxide in the form of  $Al_2O_3-Ag$ /water, has the potential to decrease skin friction while maintaining heat transfer characteristics comparable to that of  $Ag$ /water nanofluid. The findings in this publication are new and will be useful to boundary layer flow researchers. It can also be applied as a guideline for experimental investigations with the goal of reducing the cost of operation.

## 1. Introduction

The convective heat transfer flow on the surface of a sphere is an essential topic to examine. Because of its contributions in engineering and industrial applications such as spherical gas storage tanks, food processing and storage, spherical vessel insulation, thermal insulation of buildings, spherical solar energy generator and numerous electronic components that are almost spherical. Since conventional heat transfer fluids such as oil, water, and ethylene glycol blends are less efficient at transferring heat, using nanofluids can improve thermal conductivity by fluid flow, which is the

\* Corresponding author.

E-mail address: [izual@dhu.edu.my](mailto:izual@dhu.edu.my) (Nik Mohd Izual Nik Ibrahim)

<https://doi.org/10.37934/arnht.21.1.2638>

heat transfer coefficient between the medium of heat transfer and the heat transfer surface [1]. Choi from Argonne National Laboratory first proposed the notion of "nanofluids" in 1995, referring to the stable suspension formed by suspending nanoparticles of metal, metallic oxide, or non-metallic with average diameters smaller than 100 nm in a base fluid [2]. Furthermore, other researchers published additional papers on the boundary layer flow in a nanofluid. Sandhya *et al.*, [3] investigated the cooling system of an automotive radiator that use 40% ethylene glycol and 60% water with volume concentrations of  $TiO_2$  nano powder of 0.1%, 0.3%, and 0.5%. Mahat *et al.*, [4] studied the effect of viscous dissipation on mixed convection flow of viscoelastic nanofluid through a horizontal circular cylinder. Mohamed *et al.*, [5] presented the mathematical modelling of mixed convection boundary layer flow and heat transfer on a solid sphere submerged in a nanofluid with viscous dissipation effects.

It is considered that the use of nanofluid still has economic disadvantages, so researchers are exploring for materials that are regarded to be capable of covering it. Hybrid nanofluids are a new type of heat transfer nanofluid created by dispersing two types of nanoparticles in an ordinary heat transfer fluid [6]. Hybrid nanofluids have better thermophysical properties than standard heat transfer fluids (oil, water, and ethylene glycol) and mono nanofluids in thermal processes [7].

Consider the flow of fluid on a sphere, numerous studies on the flow have been completed by researchers, Kasim *et al.*, [8] and Mohamed *et al.*, [9] who studied the Free convection boundary layer flow on a solid sphere, have found that the increase of Prandtl number  $Pr$  results in the decrease of thermal boundary layer thickness and its velocity profile. Based on an evaluation of the literature and the opinions of convection on a sphere of several researchers, focus with Newtonian heating by Salleh *et al.*, [10], Flow of viscoelastic fluid by Kasim *et al.*, [11]. Flow in porous medium by Rashad [12]. Flow in a micropolar fluid by Alkasasbeh *et al.*, [13].

Recent studies of fluid flow on a sphere in hybrid nanofluid including the works from Swalmeh [14] who reported that the nanoparticle volume fraction increases, as do the values of the local Nusselt number, the skin friction coefficient, the velocity and temperature profile and also Fe-Graphene oxide/water hybrid nanofluid has a higher temperature and velocity profile compared with Fe/water nanofluid. El-Zahar *et al.*, [15] found that Surface shear stresses, the velocity distribution and temperature distribution of hybrid nanofluid ( $TiO_2$ -Ag/water) are larger than the base fluid.

It is worth mentioning that convective heat transfer on a sphere is still an interesting topic to explore. Therefore, the purpose of the present study is to investigate the mixed convection boundary layer flow over on a Sphere in  $Al_2O_3$ -Ag/Water Hybrid Nanofluid with Viscous Dissipation. The governing Partial Differential Equations (PDEs) are numerically solved, and the change of relevant physical characteristics has never been done previously, hence the findings in this study are new.

## 2. Mathematical Formulations

A two-dimensional solid sphere with radius  $a$ , which is constantly heated  $T_w$ , embedded in an incompressible viscous fluid of hybrid nanofluid with ambient temperature  $T_\infty$ . Fig. 1 represents the physical model for the case. The approximation of the boundary layer is correct. In a hybrid nanofluid, the dimensional governing equations of steady mixed convection boundary layer flow on a sphere are presented [5, 16]:

$$\frac{\partial}{\partial \bar{x}}(\bar{r}\bar{u}) + \frac{\partial}{\partial \bar{y}}(\bar{r}\bar{v}) = 0 \quad (1)$$

$$\bar{u} \frac{\partial \bar{u}}{\partial \bar{x}} + \bar{v} \frac{\partial \bar{u}}{\partial \bar{y}} = \bar{u}_e \frac{d\bar{u}_e}{d\bar{x}} + \frac{\mu_{hnf}}{\rho_{hnf}} \frac{\partial^2 \bar{u}}{\partial \bar{y}^2} + \frac{(\rho\beta)_{hnf}}{\rho_{hnf}} g(T - T_\infty) \sin \frac{\bar{x}}{a} \quad (2)$$

$$\bar{u} \frac{\partial T}{\partial \bar{x}} + \bar{v} \frac{\partial T}{\partial \bar{y}} = \frac{k_{hnf}}{(\rho C_p)_{hnf}} \frac{\partial^2 T}{\partial \bar{y}^2} + \frac{\mu_{hnf}}{(\rho C_p)_{hnf}} \left( \frac{\partial \bar{u}}{\partial \bar{y}} \right)^2 \quad (3)$$

subjected to the boundary condition:

$$\begin{aligned} \bar{u}(\bar{x}, 0) = \bar{v}(\bar{x}, 0) = 0 \quad T(\bar{x}, 0) = T_w \\ \bar{u}(\bar{x}, \infty) \rightarrow \bar{u}_e, \quad T(\bar{x}, \infty) \rightarrow T_\infty \end{aligned} \quad (4)$$

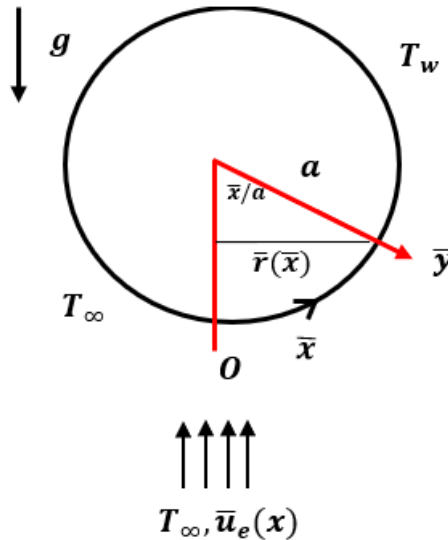


**Fig. 1.** Physical illustration of the mixed convection coordinate system on a sphere [5, 17]

where  $\bar{u}$  and  $\bar{v}$  are the velocity components along the  $\bar{x}$  and  $\bar{y}$  axes, respectively.  $\bar{u}_e$  is external velocity.  $\mu_{hnf}$  is the dynamic viscosity of hybrid nanofluid,  $\rho_{hnf}$  is the hybrid nanofluid density,  $g$  is the gravity acceleration,  $\beta_{hnf}$  is the hybrid nanofluid thermal expansion,  $T$  denotes the local temperature,  $(\rho C_p)_{hnf}$  is the heat capacity of hybrid nanofluid,  $\nu_{hnf}$  is the kinematic viscosity of hybrid nanofluid and lastly,  $k_{hnf}$  is the thermal conductivity of hybrid nanofluid which can be presented from earlier studies [18, 19-20]:

$$\begin{aligned} \nu_{hnf} &= \frac{\mu_{hnf}}{\rho_{hnf}}, \quad \mu_{hnf} = \frac{\mu_f}{(1 - \phi_1)^{2.5}(1 - \phi_2)^{2.5}}, \\ \rho_{hnf} &= (1 - \phi_2)[(1 - \phi_1)\rho_f + \phi_1\rho_{s1}] + \phi_2\rho_{s2}, \\ (\rho\beta)_{hnf} &= (1 - \phi_2)[(1 - \phi_1)(\rho\beta)_f + \phi_1(\rho\beta)_{s1}] + \phi_2(\rho\beta)_{s2}, \\ (\rho C_p)_{hnf} &= (1 - \phi_2)[(1 - \phi_1)(\rho C_p)_f + \phi_1(\rho C_p)_{s1}] + \phi_2(\rho C_p)_{s2}, \\ \frac{k_{hnf}}{k_{bf}} &= \frac{k_{s2} + 2k_{bf} - 2\phi_2(k_{bf} - k_{s2})}{k_{s2} + 2k_{bf} + \phi_2(k_{bf} - k_{s2})}, \quad \frac{k_{bf}}{k_f} = \frac{k_{s1} + 2k_f - 2\phi_1(k_f - k_{s1})}{k_{s1} + 2k_f + \phi_1(k_f - k_{s1})} \end{aligned}$$

The subscript  $_{hnf, f, s1}$  and  $_{s2}$  represent the physical attributes of hybrid nanofluid, base fluid, alumina  $Al_2O_3$  nanoparticle, and silver  $Ag$  nanoparticle, respectively. In the present study, a 0.06 vol. solid nanoparticle of  $Ag$  ( $\phi_2=0.06$ ) is mixed with a water-based fluid to create  $Ag$ /water nanofluid. Meanwhile, 0.1 vol. solid nanoparticle of  $Al_2O_3$  ( $\phi_1=0.1$ ) is added with  $Ag$ /water nanofluid to form the  $Al_2O_3$ - $Ag$ /water hybrid nanofluid.

The governing non-dimensional variables are introduced:

$$x = \frac{\bar{x}}{a}, \quad y = Re^{1/2} \frac{\bar{y}}{a}, \quad u = \frac{\bar{u}}{u_\infty}, \quad r = \frac{\bar{r}}{a}, \quad v = Re^{1/2} \frac{\bar{v}}{u_\infty},$$

$$\theta(\eta) = \frac{T - T_\infty}{T_w - T_\infty}, \quad \bar{u}_e(x) = \frac{3}{2} u_\infty \sin\left(\frac{\bar{x}}{a}\right), \quad (5)$$

Using Eq. (5), Eqs. (1–3) becomes

$$\frac{\partial}{\partial x}(ru) + \frac{\partial}{\partial y}(rv) = 0 \quad (6)$$

$$u \frac{\partial u}{\partial x} + v \frac{\partial u}{\partial y} = u_e \frac{du_e}{dx} + \frac{v_{hnf}}{v_f} \frac{\partial^2 u}{\partial y^2} + \frac{(\rho\beta)_{hnf}}{\rho_{hnf}\beta_f} \lambda \theta \sin x \quad (7)$$

$$u \frac{\partial \theta}{\partial x} + v \frac{\partial \theta}{\partial y} = \frac{k_{hnf}}{v_f(\rho C_p)_{hnf}} \frac{\partial^2 \theta}{\partial y^2} + \frac{v_{hnf}}{v_f} \frac{\rho_{hnf}(C_p)_f}{(\rho C_p)_{hnf}} Ec \left[ \frac{\partial u}{\partial y} \right]^2 \quad (8)$$

subject to boundary conditions

$$u(x, 0) = 0, \quad v(x, 0) = 0, \quad \theta(x, 0) = 1,$$

$$u(x, \infty) \rightarrow u_e, \quad \theta(x, \infty) \rightarrow 0 \quad (9)$$

where  $\theta$  denotes the rescale dimensionless temperature of the hybrid nanofluid and  $Gr, Re$ , and  $Ec$  represent the Grashof, Reynold, and Eckert numbers, respectively.

$$Gr = \frac{g\beta_f(T_w - T_\infty)a^3}{v_f^2}, \quad Re = \frac{u_\infty a}{v_f}, \quad Ec = \frac{U_\infty^2}{c_p(T_w - T_\infty)}, \quad \lambda = \frac{Gr}{Re^2}$$

Note that the  $\lambda > 0$  and  $\lambda < 0$  refers to the assisting flow and the opposing flow, respectively. To solve eqs. (6–8), the following function are introduced:

$$\psi = xf(x, y), \quad \theta = \theta(x, y) \quad (10)$$

where  $\psi$  is the stream function which defined as

$$u = \frac{\partial \psi}{\partial y} \quad \text{and} \quad v = -\frac{\partial \psi}{\partial x}$$

Further, the velocity profile and temperature distributions can be calculated using the following equations:

$$u = f'(x, y), \quad \theta = \theta(x, y) \quad (11)$$

Substituting Eq. (10) into Eqs. (6–8), the following partial differential equations (PDEs) are obtained the momentum and energy equations:

$$\frac{v_{hnf}}{v_f} \frac{\partial^3 f}{\partial y^3} - \left(\frac{\partial f}{\partial y}\right)^2 + \left[1 + x \frac{\cos x}{\sin x}\right] f \frac{\partial^2 f}{\partial y^2} + \left[\frac{9}{4} \cos x + \frac{(\rho\beta)_{hnf}}{\rho_{hnf}\beta_f} \lambda\theta\right] \frac{\sin x}{x} = x \left[\frac{\partial f}{\partial y} \frac{\partial^2 f}{\partial x \partial y} - \frac{\partial f}{\partial x} \frac{\partial^2 f}{\partial y^2}\right] \quad (12)$$

$$\frac{k_{hnf}(\rho C_p)_f}{k_f(\rho C_p)_{hnf}} \frac{1}{Pr} \frac{\partial^2 \theta}{\partial y^2} + \left[1 + x \frac{\cos x}{\sin x}\right] f \frac{\partial \theta}{\partial y} = x \left[\frac{\partial f}{\partial y} \frac{\partial \theta}{\partial x} - \frac{\partial f}{\partial x} \frac{\partial \theta}{\partial y}\right] - \left[x^2 Ec \frac{v_{hnf}}{v_f} \frac{\rho_{hnf}(C_p)_f}{(\rho C_p)_{hnf}} \left(\frac{\partial^2 f}{\partial y^2}\right)^2\right] \quad (13)$$

where  $Pr = \frac{v_f(\rho C_p)_f}{k_f}$  is the Prandtl number.

The physical quantities of importance are the local Nusselt number,  $Nu_x$  and the skin friction coefficient,  $C_f$ . Which are provided by:

$$Nu_x = \frac{aq_w}{k_f(T_w - T_\infty)}, \quad C_f = \frac{\tau_w}{\rho_f u_\infty^2} \quad (14)$$

The surface shear stress  $\tau_w$  and the surface heat flux  $q_w$  are calculated as:

$$\tau_w = \mu_{hnf} \left[\frac{\partial \bar{u}}{\partial \bar{y}}\right]_{\bar{y}=0}, \quad q_w = -k_{hnf} \left[\frac{\partial T}{\partial \bar{y}}\right]_{\bar{y}=0} \quad (15)$$

with the thermal conductivity,  $k$ . Eq. (5) and Eq. (10) provide:

$$C_f Re_x^{1/2} = \frac{1}{(1-\phi_1)^{2.5}(1-\phi_2)^{2.5}} \left(x \frac{\partial^2 f}{\partial y^2}\right)_{\bar{y}=0} \quad \text{and} \quad Nu_x Re_x^{1/2} = -\frac{k_{hnf}}{k_f} \left(\frac{\partial \theta}{\partial y}\right)_{\bar{y}=0} \quad (16)$$

Other hybrid nanofluid quantities are listed below [23]:

$i. \quad \frac{v_{hnf}}{v_f} = \frac{1}{(1-\phi_1)^{2.5}(1-\phi_2)^{2.5}(1-\phi_2)[(1-\phi_1) + \phi_1(\rho_{s1}/\rho_f)] + \phi_2(\rho_{s2}/\rho_f)}$
$ii. \quad \frac{(\rho\beta)_{hnf}}{\rho_{hnf}\beta_f} = \frac{(1-\phi_2)[(1-\phi_1)\rho_f + \phi_1(\rho\beta)_{s1}/\beta_f] + \phi_2(\rho\beta)_{s2}/\beta_f}{(1-\phi_2)[(1-\phi_1)\rho_f + \phi_1\rho_{s1}] + \phi_2\rho_{s2}}$
$iii. \quad \frac{k_{hnf}(\rho C_p)_f}{k_f(\rho C_p)_{hnf}} = \frac{k_{hnf}/k_f}{(1-\phi_2)[(1-\phi_1) + \phi_1(\rho C_p)_{s1}/(\rho C_p)_f] + \phi_2(\rho C_p)_{s2}/(\rho C_p)_f}$
$iv. \quad \frac{\rho_{hnf}(C_p)_f}{(\rho C_p)_{hnf}} = \frac{(1-\phi_2)[(1-\phi_1)\rho_f + \phi_1\rho_{s1}] + \phi_2\rho_{s2}}{(1-\phi_2)[(1-\phi_1)\rho_f + \phi_1(\rho C_p)_{s1}/(C_p)_f] + \phi_2(\rho C_p)_{s2}/(C_p)_f}$

The boundary conditions Eq. (9) become:

$$f(x, 0) = \frac{\partial f}{\partial y}(x, 0) = 0, \quad \theta(x, 0) = 1$$

$$\frac{\partial f}{\partial y}(x, \infty) \rightarrow \frac{3 \sin x}{2}, \quad \theta(x, \infty) \rightarrow 0 \quad (17)$$

### 3. Methodology

The Keller-box technique is used to solve the partial differential equations (PDEs) of Eq. (12) and Eq. (13) subject to boundary conditions Eq. (17). The Keller-box technique is a powerful implicit approach for solving non-linear parabolic PDEs. In this study, it can be used to solve nonlinear fluid flow problems. Na [21], Cebeci and Cousteix [22], and recently Mohamed [23], all provide comprehensive descriptions of the methodology. Keller-box method involves the following four steps. Firstly, to reduce the Eq. (12) and Eq. (13) subjected to the boundary conditions to a first-order system. The central finite difference procedure is applied, and it is linearized using Newton's method. Lastly, the block tridiagonal elimination method is used to solve the resulting algebraic equations after they are converted to matrix-vector form. The algorithm is numerically computed using the MATLAB programme. To obtain precise numerical results, it is worth mentioning that the boundary layer thickness is satisfied  $y_\infty = 7$  to 10 with step size  $\Delta y = 0.02$ ,  $\Delta x = 0.005$  are used.

### 4. Results

The governing Eq. (12) and Eq. (13) with parameters considered, namely mixed convection parameter  $\lambda$ , Eckert number  $Ec$ , Prandtl number  $Pr$  and the quantities of hybrid nanofluid. The reduced Nusselt number comparison values on the surface body have been predicted. It is discovered that there is a very excellent correlation between the results of the two researchers. Table 1 shows the values of thermophysical properties of water and nanoparticles [24]. Table 2 presents the comparison between the present results with the previously reported results by Nazar [25] and Mohamed [26] for various value of mixed parameter  $\lambda$  when  $\phi_1 = \phi_2 = Ec = 0$  and  $Pr = 0.7$ . Also, it is found that they are in a good agreement. Table 3 and 4 present the values of reduce of Nusselt number and reduce skin friction coefficient respectively for various values of surface on sphere  $x$  and mixed parameter  $\lambda$  when  $Pr = 7$  and  $Ec = 0.1$ . In Tables 3 and 4, the fluid flow in the assisting flow and opposing flow differs in experiencing a separation point. As the fluid velocity is high, the assisting flow occurs, and vice versa when opposing flow exists. Pressure decreases when flow passes away the front side of the cylinder. The flow is considered to have separated when the velocity gradient at the surface becomes zero. Backflow may take place as the flow passes through this separation point. Bernoulli's equation relates the increase in velocity to a drop in pressure [27]. Opposing flow,  $\lambda = -1.5, -1.0$  and  $-0.5$ , separation point occurs at  $x = 80^\circ, 90^\circ$  and  $100^\circ$  respectively. Likewise with assisting flow,  $\lambda = 0.5, 1.0$  and  $1.5$  separation occur at  $x = 110^\circ, 120^\circ$  and  $120^\circ$  respectively.

**Table 1**  
 Water and nanoparticle thermophysical characteristics [24]

Physical Properties	Water ( <i>f</i> )	$Al_2O_3$ ( $\phi_1$ )	$Ag$ ( $\phi_2$ )	$TiO_2$	<i>Cu</i>
$\rho$ (kg/m <sup>3</sup> )	997	3970	10500	4250	8933
$C_p$ (J/kg.K)	4179	765	235	686.2	385
$k$ (W/m.K)	0.613	40	429	8.95	400

**Table 2**

Value of  $Nu_x Re_x^{-1/2}$  in comparison to previously reported findings for various values of  $x$  and  $\lambda$  when  $\phi_1 = \phi_2, Pr = 0.7, Ec = 0$

$x/\lambda$	-1.0			0			1.0		
	Nazar [25]	Mohamed [26]	Present	Nazar [25]	Mohamed [26]	Present	Nazar [25]	Mohamed [26]	Present
0°	0.7870	0.7858	0.7858	0.8162	0.8150	0.8150	0.8463	0.8406	0.8406
10°	0.7818	0.7809	0.7809	0.8112	0.8103	0.8103	0.8371	0.8362	0.8362
20°	0.7669	0.7615	0.7666	0.7974	0.7967	0.7969	0.8239	0.8232	0.8235
30°	0.7422	0.7419	0.7424	0.7746	0.7741	0.7739	0.8024	0.8018	0.8022
40°	0.7076	0.7074	0.7085	0.7429	0.7425	0.7433	0.7725	0.7721	0.7728
50°	0.6624	0.6624	0.6639	0.7022	0.7032	0.7029	0.7345	0.7354	0.7351
60°	0.6055	0.6072	0.6078	0.6525	0.6521	0.6536	0.6887	0.6897	0.6897
70°	0.5334	0.5356	0.5366	0.5934	0.5946	0.5946	0.6352	0.6346	0.6363
80°	0.4342	0.4375	0.4398	0.5236	0.5249	0.5254	0.5742	0.5753	0.5758
90°				0.4398	0.4413	0.4419	0.5060	0.5071	0.5076
100°				0.3263	0.3284	0.3286	0.4304	0.4313	0.4323
110°							0.3458	0.3466	0.3483
120°							0.2442	0.2485	0.2494

**Table 3**

Value of  $Nu_x Re_x^{-1/2}$  in comparison to previously reported findings for various values of  $x$  and  $\lambda$  when  $\phi_1 = \phi_2, Pr = 7$  and  $Ec = 0.1$

$x/\lambda$	-1.5	-1.0	-0.5	0.0	0.5	1.0	1.5
0°	1.8323	1.8537	1.8742	1.8940	1.9130	1.9313	1.9491
10°	1.8004	1.8212	1.8410	1.8600	1.8782	1.8958	1.9126
20°	1.7110	1.7299	1.7477	1.7645	1.7804	1.7955	1.8098
30°	1.5757	1.5917	1.6063	1.6196	1.6366	1.6479	1.6533
40°	1.4163	1.4289	1.4396	1.4486	1.4506	1.4565	1.4671
50°	1.2407	1.2501	1.2567	1.2608	1.2626	1.2627	1.2611
60°	1.0681	1.0761	1.0793	1.0789	1.0755	1.0694	1.0608
70°	0.9037	0.9158	0.9194	0.9166	0.9089	0.8973	0.8827
80°	0.7288	0.7648	0.7777	0.7780	0.7699	0.7554	0.7358
90°		0.5713	0.6369	0.6557	0.6549	0.6425	0.6220
100°			0.3247	0.5161	0.5512	0.5490	0.5337
110°					0.3993	0.4526	0.4567
120°						0.3015	0.3722

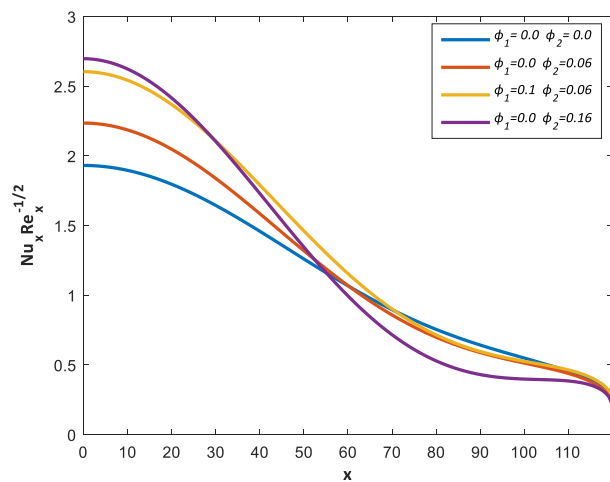
**Table 4**

Values of  $C_f Re_x^{1/2}$  in comparison to previously reported findings for various values of  $x$  and  $\lambda$  when  $\phi_1 = \phi_2$ ,  $Pr = 7$  and  $Ec = 0.1$

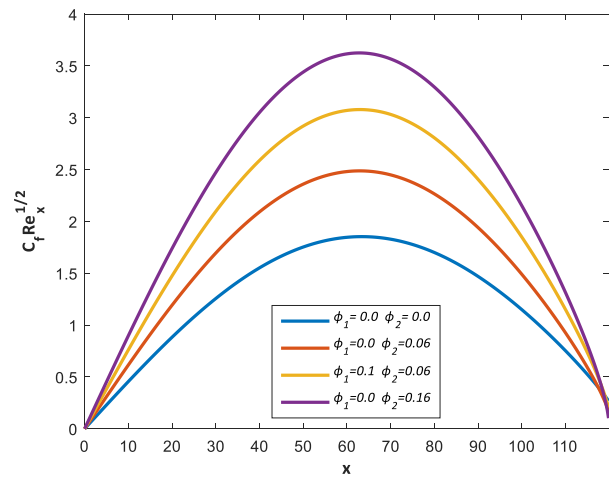
$x/\lambda$	-1.5	-1.0	-0.5	0.0	0.5	1.0	1.5
0°	0	0	0	0	0	0	0
10°	0.3530	0.3747	0.3959	0.4168	0.4372	0.4574	0.4773
20°	0.6750	0.7189	0.7619	0.8041	0.8455	0.8862	0.9263
30°	0.9370	1.0044	1.0703	1.1348	1.1889	1.2504	1.3211
40°	1.1102	1.2023	1.292	1.3794	1.4715	1.5559	1.6309
50°	1.1843	1.3048	1.4212	1.5342	1.6442	1.7516	1.8567
60°	1.1365	1.2902	1.4368	1.5779	1.7143	1.8469	1.9760
70°	0.9516	1.1480	1.3310	1.5042	1.6698	1.8293	1.9838
80°	0.5968	0.8655	1.0989	1.3120	1.5113	1.7006	1.8821
90°		0.3836	0.7275	1.0017	1.2449	1.4690	1.6800
100°			0.0513	0.5570	0.8882	1.1474	1.3932
110°					0.3837	0.7485	1.0419
120°						0.2700	0.6598

Figure 2 demonstrates the change of the volume fraction of hybrid nanofluids to reduce heat transfer along the body of the sphere. The effect of variation in  $\phi_1$  and  $\phi_2$  was discovered to be significant becomes more obvious at the stagnation point ( $x = 0$ ). It is claimed that the reduce of heat transfer decreasing along a body surface ( $x = 120^\circ$ ). The  $Al_2O_3$ -Ag/water ( $\phi_1 = 0.1$ ,  $\phi_2 = 0.06$ ) hybrid nanofluid score highest values in reduce of heat transfer compared to water-based fluid and Ag/water ( $\phi_1 = 0.0$ ,  $\phi_2 = 0.06$ ) nanofluid. These results are comparable with high-cost Ag/water ( $\phi_1 = 0.0$ ,  $\phi_2 = 0.16$ ) nanofluid. The ability of a hybrid nanofluid to transfer heat to its surrounding, which mixes metal and low-cost oxide nanoparticles, it is proved to be superior to that of premium metal nanofluid.

Figure 3 shows that, at the stagnation region ( $x = 0$ ), reduce skin friction levels are similar. The nanoparticles had no impact on friction at this point. As fluid flows through the sphere body, the reduce skin friction coefficient increases when 6 % vol. of silver nano material is added up into water-based fluid with the adding 10 % vol. of Alumina nano oxide to form the  $Al_2O_3$ -Ag/water ( $\phi_1 = 0.1$ ,  $\phi_2 = 0.06$ ) hybrid nanofluid. From Figure 3, it was discovered that the values of skin friction are varied. and then increase again without adding nano oxide ( $\phi_1 = 0.0$ ). The greatest skin friction with adding 6 % and 16 % nano material to form the Ag/water ( $\phi_1 = 0.0$ ,  $\phi_2 = 0.06$ ) and ( $\phi_1 = 0.0$ ,  $\phi_2 = 0.16$ ) nanofluid respectively. The skin friction of hybrid nanofluid  $Al_2O_3$ -Ag/water (10% nano alumina and 6 % nanofluid silver with water is smaller than of nanofluid Ag/water (0% nano alumina 16% nano sliver). Generally, the greatest skin friction occurs as the fluid flows through the surface body of sphere between  $x = 60^\circ$  and  $x = 70^\circ$ .



**Fig. 2.** Variation of  $Nu_x Re_x^{-1/2}$   $Pr = 7, Ec = 0.1$  and  $\lambda = 1$  against  $x$  for various of volume fraction



**Fig. 3.** Variation of  $C_f Re_x^{1/2}$   $Pr = 7, Ec = 0.1$  and  $\lambda = 1$  against  $x$  for various of volume fraction

The temperature profiles and velocity profiles at stagnation region ( $x = 0$ ) for various values of  $\phi_1$  and  $\phi_2$  are showed in Figures 4 and 5 respectively. More nanoparticles clearly enhance the thickness of the thermal boundary layer while decreasing the thickness of the velocity boundary layer. The addition of nanoparticles in hybrid nanofluid has increased fluid thermal conductivity, raising thermal diffusivity and increasing thermal boundary layer thickness. This is possible especially because nano oxide has a greater specific heat than nanomaterials to storage energy. The thickness of the thermal boundary layer is increased when nano oxide is added to  $Ag/water$  to generate the hybrid nanofluid.

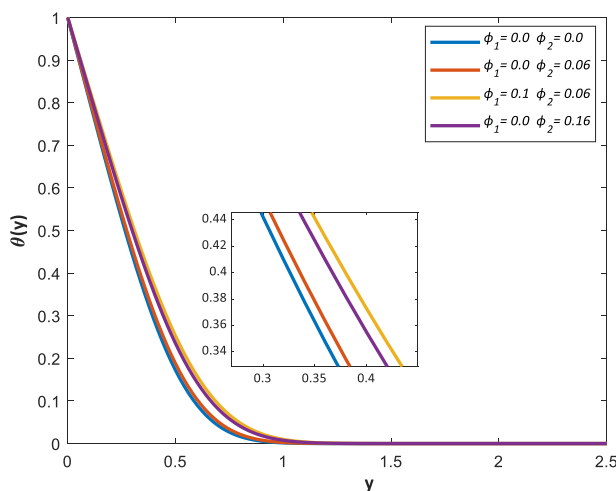


**Fig. 4.** Temperature profile  $\theta(y)$  against  $y$  for for various of volume fraction, when  $Pr = 7, Ec = 0.1$  and  $\lambda = 1$

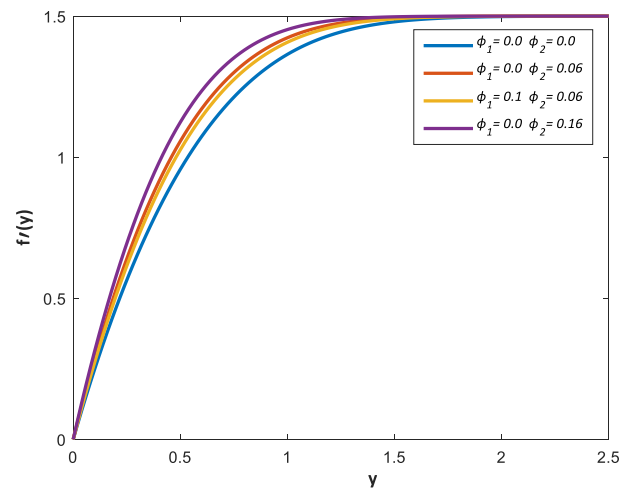


**Fig. 5.** Velocity profile  $f'(y)$  against  $y$  for various of volume fraction, when  $Pr = 7, Ec = 0.1$  and  $\lambda = 1$

Next, Figures 6 and 7 show the variation reduced Nusselt number and reduced skin friction for various values of concentration of hybrid nanofluid when  $\lambda = 1$  and  $Ec = 0.1$ . Respectively. The flow and heat transfer performance of nano oxide  $Al_2O_3$  and  $TiO_2$  with  $Ag/water$  and  $Cu/water$  to form hybrid nanofluid. From the Figure 6, it is revealed that the nanofluid of  $Ag/water$  transfers heat better than the nanofluid of  $Cu/water$ . This is due to the fact that the thermal conductivity of  $Ag$

and  $Al_2O_3$  is larger than that of  $Cu$  and  $TiO_2$ . According to Mills [28], the thermal conductivity is defined as ability of the substance to transfer energy. Figure 7, In general, the maximum skin friction is obtained when the fluid flows through the surface body of sphere between  $x = 60^\circ$  and  $x = 70^\circ$ ,  $Cu$ /water nanofluid and  $Al_2O_3$  nano oxide is found to be more efficient in reducing skin friction than  $Ag$ /water nanofluid and  $TiO_2$  nano oxide. This is due to  $Cu$  and  $Al_2O_3$  have a lower density than  $Ag$  and  $TiO_2$ .

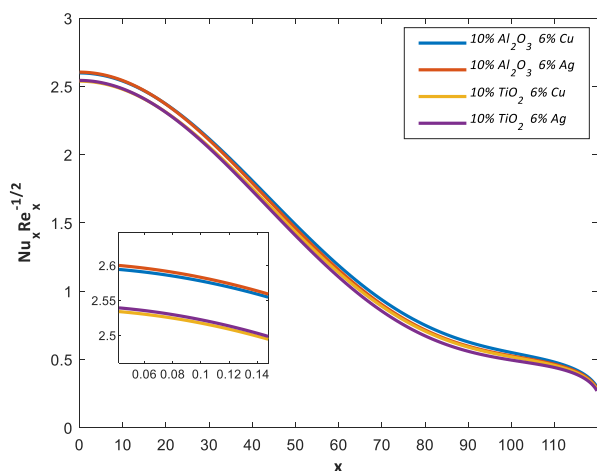


**Fig. 6.** Variation of  $Nu_x Re_x^{-1/2}$  against  $x$  for various concentration of hybrid nanofluid when  $Pr = 7$ ,  $Ec = 0.1$  and  $\lambda = 1$

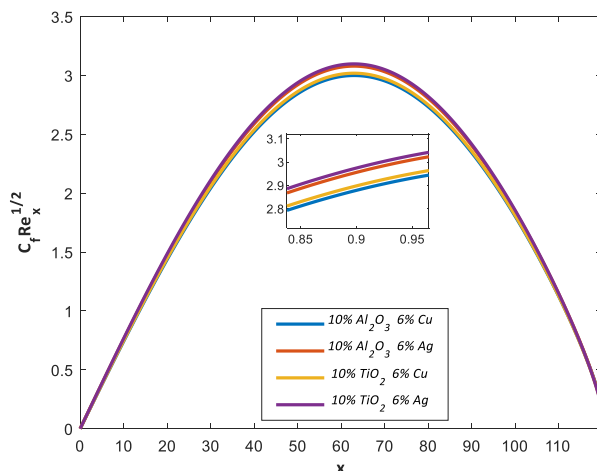


**Fig. 7.** Variation of  $C_f Re_x^{1/2}$  against  $x$  for various concentration of hybrid nanofluid when  $Pr = 7$ ,  $Ec = 0.1$  and  $\lambda = 1$

Figures 8 and 9 indicate that the reduced Nusselt number and skin friction coefficient versus  $x$  change as the Eckert number changes. The two Figures agreed that the viscous dissipation effect  $Ec$  is insignificant for the stagnation zone ( $x = 0$ ). Figure 8 shows that the viscous dissipation effect obviously influences the rate of reduced Nusselt number and it is determined by the Eckert number  $Ec$ . Increasing  $Ec$  reduces the temperature distribution without changing the fluid velocity [29]. The highest  $Ec$  number indicates a low temperature distribution on the sphere body's surface and the  $Ec$  value is also insignificant in lowering skin friction. Both statements can be viewed in fig. 8 and 9 respectively.

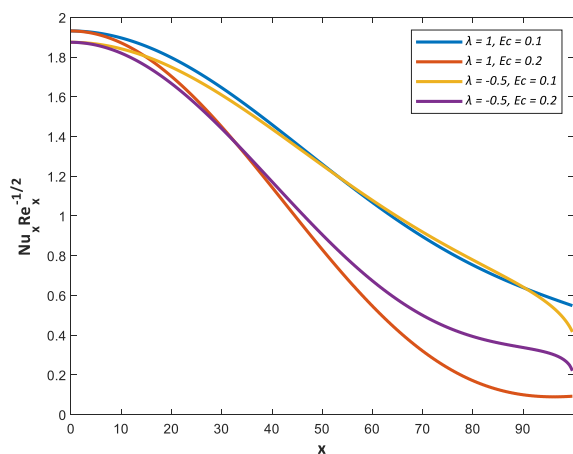


**Fig. 8.** Variation of  $Nu_x Re_x^{-1/2}$  against  $x$  for various values of  $\lambda$  and  $Ec$ ,  $\phi_1 = 0.1$  and  $\phi_2 = 0.06$

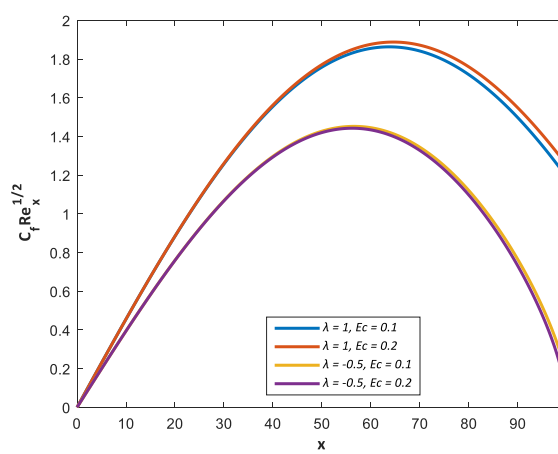


**Fig. 9.** Variation of  $C_f Re_x^{1/2}$  against  $x$  for various values of  $\lambda$  and  $Ec$ ,  $\phi_1 = 0.1$  and  $\phi_2 = 0.06$

Lastly, Figures 10 and 11 present the temperature and velocity profile against  $y$  for various of  $\lambda$ . Figure 10 shows the temperature profiles,  $\theta(y)$ , at the lower stagnation point of the solid sphere,  $x = 0$ , of hybrid nanofluid  $Al_2O_3-Ag$ /water when  $\lambda = 1$  and  $0.5$  (assisting flow) and  $\lambda = -0.1$  and  $-0.5$  (opposing flow). It is observed that the opposing flow has a thicker thermal boundary layer than the assisting flow. This may be due to the low velocity of the fluid, as a result, the effective thermal boundary layer develops are noticeably. Meanwhile, the velocity of the assisting flow is greater than that of the opposing flow, as seen in the velocity profile in figure 11.

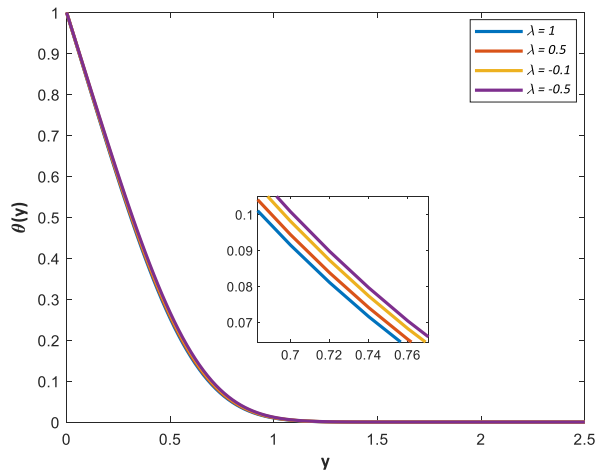


**Fig. 10.** Temperature profile  $\theta(y)$  against  $y$  for for various of  $\lambda$ ,  $\phi_1 = 0.1$  and  $\phi_2 = 0.06$

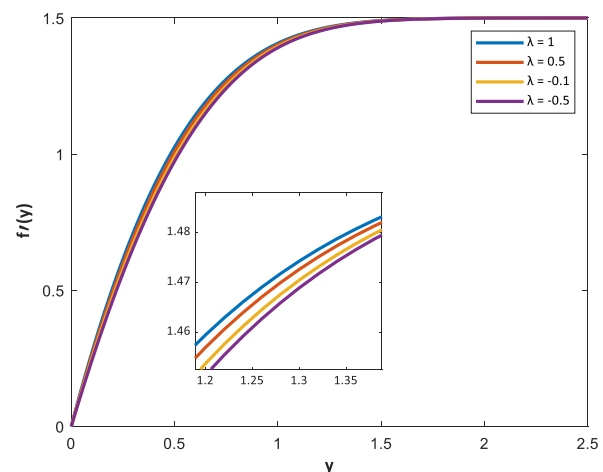


**Fig. 11.** Velocity profile  $f'(y)$  against  $y$  for for various of  $\lambda$ ,  $\phi_1 = 0.1$  and  $\phi_2 = 0.06$

## 5. Conclusions

In this study, the Keller-box technique is used to investigate the mixed convection boundary layer flow on a sphere in hybrid nanofluid. The effect of the mixed parameter  $\lambda$ , the Eckert number  $Ec$ , and the volume fractions of oxide nanoparticles and metal nanoparticles for hybrid nanofluids are observed. As a result, it is found:

- i) The ability of a hybrid nanofluid to transfer heat to its surrounding, which mixes metal and low-cost oxide nanoparticles, it is proved to be superior to that of premium metal nanofluid.
- ii) The low density of nano oxides in hybrid nanofluids, such as alumina, additionally contributes to minimizing friction between fluid and body surface.
- iii) Based on numerical analysis, the combination of nanoparticles with  $Al_2O_3-Ag$ /water hybrid nanofluid may reduce skin friction phenomena while preserving heat transfer properties comparable to  $Ag$ /water nanofluid.
- iv) The opposing flow has a thicker thermal boundary layer than the assisting flow. This could be due to the low fluid velocity, as a result, the effective thermal boundary layer develops noticeably.

Upon that, it is discovered that skin friction faced more friction in the middle of the sphere surface body, The Nusselt number, on the other hand, decreases along the body. In the field of fluid dynamics, it has been shown that an increase in the Eckert number leads to a corresponding rise in the friction coefficient during assisting flow. Conversely, in opposing flow conditions, an increase in the Eckert number results in a drop in the friction coefficient. Furthermore, it is observed that nanoparticles with high thermal conductivity, such as silver, has a high heat transfer capability.

## Acknowledgement

Authors gratefully acknowledge the financial and facilities support from the Malaysia Ministry of Education (FRGS/1/2019/STG06/ DHUAM/02/1), DRB-HICOM University of Automotive Malaysia.

## References

- [1] Tham, Leony, and Roslinda Nazar. "Mixed convection flow about a solid sphere embedded in a porous medium filled with a nanofluid." (2012): 1643-1649. <https://doi.org/10.1063/1.4823922>
- [2] Choi, S. US, and Jeffrey A. Eastman. *Enhancing thermal conductivity of fluids with nanoparticles*. No. ANL/MSD/CP-84938; CONF-951135-29. Argonne National Lab.(ANL), Argonne, IL (United States), 1995.
- [3] Devireddy, Sandhya, Chandra Sekhara Reddy Mekala, and Vasudeva Rao Veerredhi. "Improving the cooling performance of automobile radiator with ethylene glycol water based TiO<sub>2</sub> nanofluids." *International communications in heat and mass transfer* 78 (2016): 121-126. <https://doi.org/10.1016/j.icheatmasstransfer.2016.09.002>
- [4] Mahat, Rahimah, Noraihan Afiqah Rawi, Abdul Rahman Mohd Kasim, and Sharidan Shafie. "Mixed convection flow of viscoelastic nanofluid past a horizontal circular cylinder with viscous dissipation." *Sains Malaysiana* 47, no. 7 (2018): 1617-1623. <https://doi.org/10.17576/jsm-2018-4707-33>
- [5] Mohamed, Muhammad Khairul Anuar, Mohd Zuki Salleh, Anuar Ishak, and Roslinda Nazar. "Mixed convection boundary layer flow on a solid sphere in a nanofluid with the presence of viscous dissipation." *a a 2* (2020): 2. [https://doi.org/10.32802/asmsci.2020.sm26\(4.7\)](https://doi.org/10.32802/asmsci.2020.sm26(4.7))
- [6] Asim, Muhammad, and Farooq Riaz Siddiqui. "Hybrid nanofluids—next-generation fluids for spray-cooling-based thermal management of high-heat-flux devices." *Nanomaterials* 12, no. 3 (2022): 507. <https://doi.org/10.3390/nano12030507>
- [7] Kshirsagar, Dattatraya P., and M. A. Venkatesh. "A review on hybrid nanofluids for engineering applications." *Materials Today: Proceedings* 44 (2021): 744-755. <https://doi.org/10.1016/j.matpr.2020.10.637>
- [8] Kasim, Abdul Rahman Mohd, N. F. Mohammad, and S. Sharidan. "Natural convection boundary layer flow of a viscoelastic fluid on solid sphere with Newtonian heating." *International Journal of Physical and Mathematical Sciences* 6, no. 4 (2012): 410-415. <http://dx.doi.org/10.5281/zenodo.1328964>
- [9] Mohamed, Muhammad Khairul Anuar, Nor Aida Zuraimi Md Noar, Mohd Zuki Salleh, and Anuar Ishak. "Free convection boundary layer flow on a solid sphere in a nanofluid with viscous dissipation." *Malaysian Journal of Fundamental and Applied Sciences* 15, no. 3 (2019): 381-388. <https://doi.org/10.11113/mjfas.v15n3.1183>
- [10] Salleh, M. Z., R. Nazar, and I. Pop. "Mixed convection boundary layer flow from a solid sphere with Newtonian heating in a micropolar fluid." *SRX Physics* 2010 (2010). <https://doi.org/10.3814/2010/736039>
- [11] Kasim, A. R. M., N. F. Mohammad, A. Aurangzaib, and S. Shafie. "Natural convection boundary layer flow past a sphere with constant heat flux in viscoelastic fluid." *Jurnal Teknologi* 62, no. 3 (2013): 27-32. <https://doi.org/10.11113/jt.v62.1885>
- [12] Rashad, A. M. "Natural convection boundary layer flow along a sphere embedded in a porous medium filled with a nanofluid." *Latin American applied research* 44, no. 2 (2014): 149-157. <https://doi.org/10.52292/j.laar.2014.433>
- [13] Alkasasbeh, Hamzeh Taha, Mohd Zuki Salleh, Razman Mat Tahar, Roslinda Nazar, and Ioan Pop. "Free convection boundary layer flow on a solid sphere with convective boundary conditions in a micropolar fluid." *World Applied Sciences Journal* 32, no. 9 (2014): 1942-1951. <https://doi.org/10.1063/1.4882469>
- [14] Swalmeh, Mohammed Zaki. "Numerical solutions of hybrid nanofluids flow via free convection over a solid sphere." *Journal of Advanced Research in Fluid Mechanics and Thermal Sciences* 83, no. 1 (2021): 34-45. <https://doi.org/10.37934/arfmts.83.1.3445>
- [15] El-Zahar, Essam R., Abd El Nasser Mahdy, Ahmed M. Rashad, Wafaa Saad, and Laila F. Seddek. "Unsteady MHD mixed convection flow of Non-Newtonian Casson hybrid nanofluid in the stagnation zone of sphere spinning impulsively." *Fluids* 6, no. 6 (2021): 197. <https://doi.org/10.3390/fluids6060197>
- [16] Mohamed, Muhammad Khairul Anuar, Anuar Mohd Ishak, Ioan Pop, Nurul Farahain Mohammad, and Siti Khuzaimah Soid. "Free convection boundary layer flow from a vertical truncated cone in a hybrid nanofluid." *Malaysian Journal of Fundamental and Applied Sciences* 18, no. 2 (2022): 257-270. <https://doi.org/10.11113/mjfas.v18n2.2410>
- [17] Tham, Leony, and Roslinda Nazar. "Mixed convection flow about a solid sphere with a constant surface heat flux embedded in a porous medium filled with a nanofluid." In *AIP Conference Proceedings*, vol. 1557, no. 1, pp. 291-295. American Institute of Physics, 2013. <https://doi.org/10.1063/1.4823922>
- [18] Devi, Suriya Uma, and SP Anjali Devi. "Heat transfer enhancement of Cu- $\text{Al}_2\text{O}_3$ /water hybrid nanofluid flow over a stretching sheet." *Journal of the Nigerian Mathematical Society* 36, no. 2 (2017): 419-433. <https://ojs.ictp.it/jnms/index.php/jnms/article/view/147>.

- [19] Mohamed, Muhammad Khairul Anuar, Huei Ruy Ong, Hamzah Taha Alkasasbeh, and Mohd Zuki Salleh. "Heat transfer of ag-Al<sub>2</sub>O<sub>3</sub>/water hybrid nanofluid on a stagnation point flow over a stretching sheet with newtonian heating." In *Journal of Physics: Conference Series*, vol. 1529, no. 4, p. 042085. IOP Publishing, 2020. <https://doi.org/10.1088/1742-6596/1529/4/042085>
- [20] Raju, S. Suresh Kumar. "Dynamical dissipative and radiative flow of comparative an irreversibility analysis of micropolar and hybrid nanofluid over a Joule heating inclined channel." *Scientific Reports* 13, no. 1 (2023): 5356. <https://doi.org/10.1038/s41598-023-31920-1>
- [21] Na, T. Y. "Computational methods in engineering." *Boundary value problems. ACADEMIC PRESS: A Subsidiary of Harcourt Brace Jovanovich, Publishers, New York, London, Toronto, Sydney, San Francisco* (1979): 310.
- [22] Cousteix, T. Cebeci J., and J. Cebeci. "Modeling and computation of boundary-layer flows." *Berlin, Germany: Springer* (2005). [https://doi.org/10.1007/3-540-27361-1\\_5](https://doi.org/10.1007/3-540-27361-1_5)
- [23] Mohamed, Muhammad Khairul Anuar, Mohd Zuki Salleh, Fadhilah Che Jamil, and Ong Huei. "Free convection boundary layer flow over a horizontal circular cylinder in Al<sub>2</sub>O<sub>3</sub>-Ag/water hybrid nanofluid with viscous dissipation." *Malaysian Journal of Fundamental and Applied Sciences* 17, no. 1 (2021): 20-25. <https://doi.org/10.11113/mjfas.v17n1.1964>
- [24] Das, Sarit K., Stephen US Choi, Wenhua Yu, and T. Pradeep. "Nanofluids-Science and Technology. A John Wiley & Sons." *Inc., Hoboken* (2008). <https://doi.org/10.1002/9780470180693>
- [25] Nazar, Roslinda, Norsarahaida Amin, and Ioan Pop. "Mixed convection boundary layer flow about an isothermal sphere in a micropolar fluid." *International journal of thermal sciences* 42, no. 3 (2003): 283-293. [https://doi.org/10.1016/S1290-0729\(02\)00027-3](https://doi.org/10.1016/S1290-0729(02)00027-3)
- [26] Mohamed, Muhammad Khairul Anuar, Norhafizah Mohd Sarif, N. A. Z. M. Noar, Mohd Zuki Salleh, and Anuar Ishak. "Viscous dissipation effect on the mixed convection boundary layer flow towards solid sphere." *Trans. Sci. Technol* 3, no. 1-2 (2016): 59-67. [https://www.transectscience.org/pdfs/vol3/no1\\_2/31](https://www.transectscience.org/pdfs/vol3/no1_2/31)
- [27] Schäfle, Claudia, and Christian Kautz. "Student reasoning in hydrodynamics: Bernoulli's principle versus the continuity equation." *Physical Review Physics Education Research* 17, no. 1 (2021): 010147. <https://doi.org/10.1103/PhysRevPhysEducRes.17.010147>
- [28] Mills, Anthony. *Heat and mass transfer*. Routledge, 2018. <https://doi.org/10.4324/9780203752173>
- [29] Famakinwa, O. A., O. K. Koriko, and K. S. Adegbe. "Effects of viscous dissipation and thermal radiation on time dependent incompressible squeezing flow of CuO– Al<sub>2</sub>O<sub>3</sub>/water hybrid nanofluid between two parallel plates with variable viscosity." *Journal of Computational Mathematics and Data Science* 5 (2022): 100062. <https://doi.org/10.1016/j.icmds.2022.100062>